Atmospheric Research 174–175 (2016) 124–134

Contents lists available at ScienceDirect

Atmospheric Research

journal homepage: www.elsevier.com/locate/atmosres

A 15-year climatology of wind pattern impacts on surface ozone in Houston, Texas

Amir Hossein Souri, Yunsoo Choi *, Xiangshang Li, Alexander Kotsakis, Xun Jiang

Department of Earth and Atmospheric Sciences, University of Houston, 312 Science & Research Building 1, Houston, TX 77204, USA

ARTICLE INFO

Article history:
Received 3 December 2015
Received in revised form 5 February 2016
Accepted 9 February 2016
Available online 18 February 2016

Keywords:
Ozone
Wind pattern
Clustering
Trend analysis
Principal component analysis

ABSTRACT

Houston is recognized for its large petrochemical industrial facilities providing abundant radicals for tropospheric ozone formation. Fortunately, maximum daily 8-h average (MDA8) surface ozone concentrations have declined in Houston (-0.6 ± 0.3 ppbv yr^{-1}) during the summers (i.e., May to September) of 2000 to 2014, possibly due to the reductions in precursor emissions by effective control policies. However, it is also possible that changes in meteorological variables have affected ozone concentrations. This study focused on the impact of long-term wind patterns which have the highest impact on ozone in Houston. The analysis of long-term wind patterns can benefit surface ozone studies by 1) providing wind patterns that distinctly changed ozone levels, 2) investigating the frequency of patterns and the respective changes and 3) estimating ozone trends in specific wind patterns that local emissions are mostly involved, thus separating emissions impacts from meteorology to some extent. To this end, the 900-hPa flow patterns in summers of 2000 to 2014 were clustered in seven classes (C1–C7) by deploying an unsupervised partitioning method. We confirm the characteristics of the clusters from a backward trajectory analysis, monitoring networks, and a regional chemical transport model simulation. The results indicate that Houston has experienced a statistically significant downward trend (-0.6 ± 0.4 day yr^{-1}) of the cluster of weak easterly and northeasterly days (C4), when the highest fraction of ozone exceedances (MDA8 > 70 ppbv) occurred. This suggests that the reduction in ozone precursors was not the sole reason for the decrease in ozone exceedance days (-1.5 ± 0.6 day yr^{-1}). Further, to examine the efficiency of control policies intended to reduce the amount of ozone, we estimated the trend of MDA8 ozone in C4 and C5 (weak winds) days when local emissions are primarily responsible for high ambient ozone levels. Both C4 and C5 show a large reduction in the 95th percentile and summertime trends mainly due to effective control strategies. Based on the 5th percentile daytime ozone for C1 (strong southeasterly wind) in coastal sites, this study found that the cleanest air masses that Houston received became more polluted during the summer of 2000–2014 by 1–3 ppbv. Though this study focused on Houston, the analysis method presented could generally be used to estimate ozone trends in other regions where surface ozone is dominantly influenced by both wind patterns and local emissions.

1. Introduction

Tropospheric ozone (O_3) not only adversely affects human health, crop yields, and organic materials when they are exposed to high concentrations, but also acts as a greenhouse gas, directly contributing to global climate change (Seinfeld and Pandis, 2012). In addition, O_3 impacts concentrations of hydroxyl radicals (OH), thereby controlling the oxidation of many common trace gases. In the troposphere, O_3 forms photochemically from complex chemical reactions involving nitrogen oxides ($NO_x = NO + NO_2$), reactive volatile organic compounds (VOC), and OH (Sillman, 1995). Understanding the origins of surface ozone levels requires knowledge of meteorological factors (e.g., Banta et al., 2005) and emission sources (e.g., Li et al., 2016). The non-linearity of ozone production, variability in sources and sinks, and the impact of the ozone background (particularly from East Asia) have resulted in various trends across seasons and locations in the United States. Lefohn et al. (2010) analyzed surface ozone for different periods (i.e., 1980 to 2008 and 1994 to 2008) and found that the second highest annual 1-h average ozone and fourth highest daily maximum 8-h average in both rural and urban regions decreased largely during the summer. Cooper et al. (2012) found that during the summers of 1990–2010, most eastern rural regions experienced statistically significant decreases in the 95th and 50th percentiles of ozone, while the reduction in the western U.S. was minimal, especially during the springtime, possibly because of the elevated ozone levels hemispherically transported from Asia or deep stratospheric intrusions (Lin et al., 2015). More recently, during a period in which widespread reductions of NO_x and VOC anthropogenic emissions took place (1998–2013), Simon et al. (2014) found that ozone concentrations in the 95th percentile declined by 1–2 ppbv yr^{-1} in urban, suburban, and rural regions.

The Houston–Galveston–Brazoria (HGB) region is known for its large petrochemical industrial facilities and is located in a non-attainment region with respect to ozone pollution. Despite significant

* Corresponding author.
E-mail address: ychoi6@uh.edu (Y. Choi).

http://dx.doi.org/10.1016/j.atmosres.2016.02.007
0169-8095/

urbanization, governmental regulatory policies have lowered the emissions of ozone precursors. According to air pollutant emissions trend data from the National Emissions Inventory (NEI) of the US EPA (U.S. EPA, 2014) anthropogenic sources of NO_x from both stationary and mobile sources declined by 45% in the U.S. from 2000 to 2014. In addition, VOC anthropogenic emissions decreased by 16%. Although these numbers indicate a trend in the reduction of ozone precursors, comprehensive studies with supporting measurements (concentrations) need to be conducted to confirm such a trend. Due to the lack of sufficient in-situ observations of NO_2 and HCHO (a proxy for VOC reactivity), several studies have devoted themselves to the analysis of trends from satellite-based measurements (e.g., Tong et al., 2015; Choi and Souri, 2015a; Duncan et al., 2016). In the last decade, through the use of various satellites and retrieval methods, a reduction in tropospheric NO_2 in Houston has been detected by Choi et al. (2012), Russell et al. (2012), Hilboll et al. (2013), Tong et al. (2015), Choi (2014), Choi and Souri (2015b) and Duncan et al. (2016). De Smedt et al. (2010, 2015) and Choi and Souri (2015b) found that the reduction in the HCHO column over Houston was not as significant as the VOC anthropogenic emissions in Houston (Washenfelder et al., 2010) possibly resulting from biogenic emissions or climatic variabilities. An overview of NO_2 and HCHO trends seen from space is listed in Table 1.

There have been several studies devoted to examining ozone trends in Houston. In particular, Lefer et al. (2010) concluded, through the use of measurement data, that the MDA8 ozone in Houston between 1991 and 2009 decreased likely as a result of anthropogenic reductions. Zhou et al. (2014), using airborne observations from two field campaigns (2000 and 2006), found that ozone production declined by 40%–50% in the city; however, meteorological changes remain unknown. The biggest obstacle in the development of appropriate emission control policies that could mitigate the levels of ozone and the impact on consequent health and climate changes is the difficulty of quantifying the influences of long-term meteorology and emissions on changes in both ozone and its precursors. Therefore, this study is motivated by the need to understand the impact of meteorological changes on surface ozone concentrations. Among the many meteorological factors, wind fields have been proven to be the most prominent factor controlling the distribution of ozone precursors and the production rate in Houston. Although the impacts of wind patterns have been extensively studied in Houston (e.g., Darby, 2005; Banta et al., 2005; Rappenglück et al., 2008; Ngan and Byun, 2011), the time periods of these case studies were short. As far as we know, Davis et al. (1998) was the only study that used cluster analysis in a long-term study period (1981–1992) in Houston by using observations from the Houston International Airport. The study found that a majority of high daily 1-h maximum ozone events occurred during the summer months. Our work utilizes a cluster analysis in a regional-scale domain based on reanalysis data rather than sparse observations. This analysis also captures changes in the frequency of wind patterns and trends in ozone within the clusters, specifically in the summertime.

Clustering wind patterns can help us to estimate the baseline ozone (e.g., Chan and Vet, 2010) and ozone levels that are mainly governed by local emissions. Conventional methods for estimating baseline and regional background ozone (the definitions of which are presented in Berlin et al. 2013) have been based on the deployment of an isolated station, aircraft measurements (Kemball-Cook et al., 2009), or ozonesonde observations. However, these techniques are limited to short time periods or few sites. Additionally, the flat topography of Houston prevents the use of any elevated station to mitigate the effects of local emissions. Berlin et al. (2013) used principal component analysis (PCA) on MDA8 ozone, and defined the regional background as the principal component that correlates strongly with uniform ozone levels at continuous ambient monitoring stations (CAMS) operated by the Texas Commission on Environmental Quality (TCEQ). They concluded that between 1998 and 2012, the amount of regional background ozone in Houston declined dramatically (-0.92 ± 0.78 ppbv yr^{-1}) which should be considered to derive local emissions impacts on ozone trends. The goal of this study is 1) to cluster wind patterns that have distinctive impacts on surface ozone in Houston, 2) to examine the trend of wind pattern frequencies, 3) to investigate the trend of baseline ozone (i.e., from the Gulf of Mexico) in Houston and 4) to estimate the trend of ozone which was produced mainly by local emissions with the aid of the wind pattern clusters.

2. Measurements and modeling

2.1. Wind direction

Our delineation of wind patterns was mainly based on U- and V-wind components from the three-hourly National Centers for Environmental Prediction-North American Regional Reanalysis (NCEP-NARR) (Mesinger et al., 2006) with a spatial resolution of 32 km. The data analyzed for this study were gathered during the summers (i.e., May to September) of 2000 to 2014. Theoretically, winds at lower standard atmospheric levels of 900 hPa, 850 hPa, and 700 hPa were all possible choices because they were neither complicated by the surface topography nor uncorrelated with surface air pollution. Ngan and Byun (2011) used 850 hPa winds because this level was not subject to direct local influence. Nevertheless, we used 900 hPa winds which have stronger ozone-predicting capability because they are closer to the boundary layer, where the winds directly influence ozone concentrations. Lower wind levels were not considered because of the complexity and possible uncertainties of NARR surface winds. The averaged morning time data at 6:00 a.m., 9:00 a.m. and 12:00 p.m. local standard time (LST) were used to capture the main initial flow pattern, strongly affecting afternoon ozone concentrations (a peak around ~1300–1600 LST).

2.2. In-situ surface ozone and NO_2

In-situ surface data included regular measurements from the CAMS measurement network. The network collects hourly meteorology and chemistry data. The measured parameters vary from station to station.

Table 1
Overview of ozone precursor trends in Houston seen by remote sensing. Note that the spatial subset for Houston city and the radiometric error flags might be inconsistent in the literatures.

Variable	Period	Reference	Instrument	Trend
NO_2	2005–2011	Russell et al. (2012)	Berkley OMI[a]	$-4.7\%\ yr^{-1}$
	2005–2013	Choi and Souri (2015b)	NASA OMI	$-1.7\%\ yr^{-1}$
	2005–2012	Tong et al. (2015)	NASA OMI	$-3.4\%\ yr^{-1}$
	2005–2014	Duncan et al. (2016)	NASA OMI	$-3.8\%\ yr^{-1}$
HCHO	1997–2009	De Smedt et al. (2010)	GOME[b] and SCIAMACHY[c]	$-1.1\%\ yr^{-1}$
	2005–2013	Choi and Souri (2015b)	SAO OMI	$-0.6\%\ yr^{-1}$
	2005–2014	De Smedt et al. (2015)	BIRA-IASB OMI	$-1.1\%\ yr^{-1}$

[a] Ozone Monitoring Instrument.
[b] Global Ozone Monitoring Experiment.
[c] Scanning Imaging Absorption Spectrometer for Atmospheric Chartography.

The station network in Houston is comparatively dense. The locations and statuses of these sites in which the ozone and nitrogen dioxide gases are measured are shown in the left and right panels of Fig. 1, respectively. To estimate the atmospheric chemical and physical characteristics of each wind pattern, we used all available stations during the period. However, in order to estimate ozone trends, we only included the stations that measured the gases continuously from 2000 to 2014 (i.e., number of observations >2100 days out of 2250). The monitoring sites measured NO_2 by chemiluminescence that might have a systematic bias (5–15%) (e.g., Souri et al., in press) due to interference from other reactive nitrogen species such as PAN and alkyl nitrates. Here, we assumed that absolute long-term trends of these reactive nitrogen gases were relatively smaller than NO_2, thereby no correction was applied.

2.3. Ancillary analysis

To theoretically demonstrate the influences of wind patterns on afternoon surface ozone, we used the US EPA Community Multiscale Air Quality (CMAQ) model (Byun and Schere, 2006), version 5.0.1, to simulate air quality on a 4 km domain during the summer of 2014 (i.e., May to September). Meteorological fields were simulated by the Weather Research and Forecasting (WRF) model version 3.5 (Skamarock and Klemp, 2008). Lateral boundary conditions were derived from NARR. While Eta-NAM reanalysis could provide a better spatial resolution (12 km, every 6 h) for the WRF run, Li et al. (2015) demonstrated that NARR re-analysis gave better results likely due to a higher temporal resolution (every 3 h). The chemical boundary conditions for a 4 km CMAQ run were obtained from the University of Houston air quality forecasting system (http://spock.geosc.uh.edu) from a parent domain which had 12 km grid resolution, and 150 and 134 grid cells in x–y directions covering Texas (Fig. 2 in Li et al., 2015). Among the major WRF physics options, the planetary boundary layer parameterization, which is imperative for surface ozone modeling, was set to the Yonsei University (YSU) scheme (Hong et al., 2006). Our 4 km simulation model domain covering southeast Texas consisted of 84 and 66 grid cells in the x–y directions respectively with 27 vertical layers. The emissions inventory used for the simulation was NEI-2008, which was processed with the Sparse Matrix Operator Kernel Emissions (SMOKE) v3.1 and the MOVES (Motor Vehicle Emission Simulator). Emissions from natural sources were calculated with BEIS3 (Biogenic Emission Inventory System version 3). The details of the model setups and validations against the atmospheric chemical and meteorological measurements are described in previous studies by Czader et al. (2015), Li et al. (2015), Pan et al. (2015), and Souri et al. (in press).

3. Methodology

3.1. Wind pattern clustering

The purpose of wind pattern clustering is to group the selected days in such a way that the days in the same group share a similar pattern of certain meteorological variable(s). To classify proper wind patterns, an appropriate classification method and underlying variable(s) should be selected. Classification methods generally fall into two categories: supervised (i.e., having some priori knowledge, expectations and prototypes for each cluster) (e.g., Souri and Vajedian, 2015) and unsupervised (i.e., without providing prototypes) methods. The most commonly used unsupervised method is the nonhierarchical K-means method (Huth et al., 2008), which was implemented for this study. The domain for the clustering covered eastern Texas, southern Oklahoma, southern Arkansas, southern Mississippi, and all of Louisiana, including 37×47 (1739) grid cells over 2250 days (daily data in five months of May to September). To reduce redundancy, we applied PCA to the 900 hPa U and V components (i.e., $1739 \times 2 \times 2550$). Only 40 PCs were extracted as candidate components. Next, we used the K-means clustering method to employ an iterative algorithm that minimizes the sum of distances (here, the squared Euclidean distance) from each day to its cluster centroids with respect to all of the clusters. This method moved days between clusters until the sum could no longer be reduced. Similar to other types of numerical minimizations, the solutions that K-means obtains are determined by the starting points. Thereby, it is probable for K-means to converge to a local minimum. In this study, therefore, we repeated clustering 1000 times, each with a new set of initial points, and our method returned a solution with the lowest value for the sum of the distances.

3.2. Backward trajectory analysis

We used the Hybrid Single-Particle Langrangian Integrated Trajectory Model (HYSPLIT, version 4), developed by the USA NOAA Air Resources Laboratory (Stein et al., 2015), to retrieve three-day backward trajectory paths arriving at 12:00 and 18:00 UTC. The trajectories had

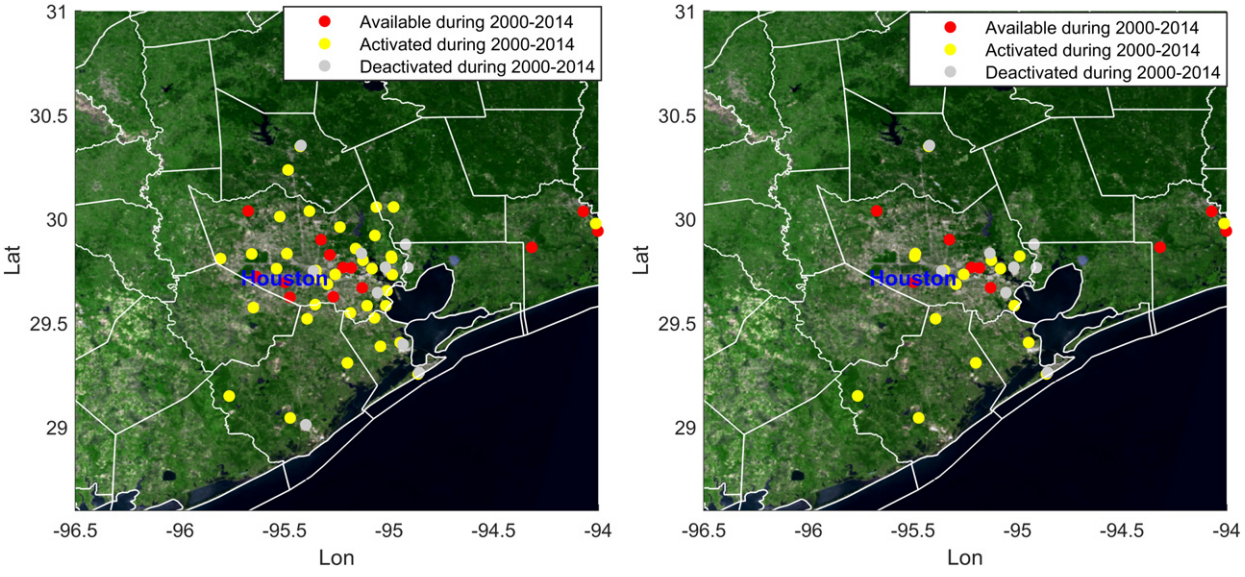

Fig. 1. The MODIS true colors showing the locations and statuses of the CAMS ozone sites (in the left panel) and the locations and statuses of NO_2 monitors from 2000 to 2014 (in the right panel). The red sites denote stations that continuously measured the species during that period.

ending points at ozone CAMS stations at 15 m above ground level in Houston from 2000 to 2014. The objective of this analysis was to check the pattern of air masses for each cluster during this period. The meteorological data used for the analysis were NARR fields.

3.3. Long-term trend analysis

In the analysis of trends in summertime cluster frequency, ozone, and NO_2, we used the ordinary linear least squares method and noted the differences between the lower and upper confidence boundaries of the computed trends (95%) for the normal distribution. We captured the trends of the 95th and 5th ozone quantiles using a quantile regression model (Koenker and Hallock, 2001). To investigate whether a trend is statistically significant, we performed a bootstrap technique with 2000 iterations on the trend estimator. Using a 95% bootstrap confidence interval, we called a trend statistically significant if and only if the confidence interval did not include zero.

4. Results and discussions

4.1. Present-day status of anthropogenic emissions, NO_2 and O_3

Prior to discussing wind pattern clustering and its impact on ozone, this section focuses on changes in anthropogenic VOC and NO_x emissions, and ambient levels of ozone and NO_2 from 2000 to 2014. As outlined earlier, anthropogenic VOC and NO_x emissions were largely reduced in the U.S. However, the changes in anthropogenic emissions are inconsistent across the U.S.; accordingly, we calculated the trends in MACCity anthropogenic NO_x and HCHO (a proxy for VOC reactivity) emissions (Lamarque et al., 2010) in the HGB region and found a 64% reduction in NO_x and a 69% reduction in HCHO during the period. This is significant, since Houston comprises a large number of industrial facilities. Fig. 3 depicts NO_x and VOC emissions from point sources (i.e., industrial facilities in Houston) from the TCEQ 2013 Point Source Emissions Inventory (PSEI). According to the data, a significant amount of VOC emissions originate in the Houston Ship Channel and Mont Belvieu, where large petrochemical industrial facilities are located. The importance of VOC point sources on ozone production in the region has been extensively studied (e.g., Jobson et al., 2004; Washenfelder et al., 2010). In particular, Washenfelder et al. (2010), using NOAA WP-3D aircraft measurements taken on 26 Sept. 2006, calculated the OH reactivity of a variety of VOC species in Houston. They found that anthropogenic VOC sources, not biogenic VOC sources in this area, were the dominant contributor to ozone formation. Based on TCEQ 1999 and 2013 PSEI emissions, we found that VOC point source emissions decreased by 44% in the Houston Ship Channel. This reduction was higher than the norm of VOC emissions changes reported by EPA in the U.S. (~16% from 2000 to 2014). In addition, Choi and Souri (2015b) demonstrated that OMI HCHO declined by 5% over Houston from 2005 to 2013, while climatic effects such as accelerated photochemical reaction rates and increased biogenic isoprene emissions during the La Niña years (Fu et al., 2015; Huang et al., 2015) have increased HCHO concentrations in southeastern Texas. This emphasizes the influence of VOC reductions in Houston (especially in the Houston Ship Channel) that cancelled out possible increases in biogenic emissions.

Because of the importance of MDA8 ozone in human health standards, we calculated the episode-average MDA8 for each of the 11 stations in the summers of 2000 to 2014. Next, we evaluated the trends of summer, 95th, and 5th percentiles of MDA8 ozone. The results indicated that the trends were statistically significant at -1.5 ± 0.2 ppbv yr^{-1} and -0.6 ± 0.3 ppbv yr^{-1} for the 95th percentile and summertime ozone levels respectively. Moreover, we found that NO_2 decreased as 0.45 ± 0.04 ppbv yr^{-1} during the summertime (not shown). The ozone reduction may have resulted from reductions in

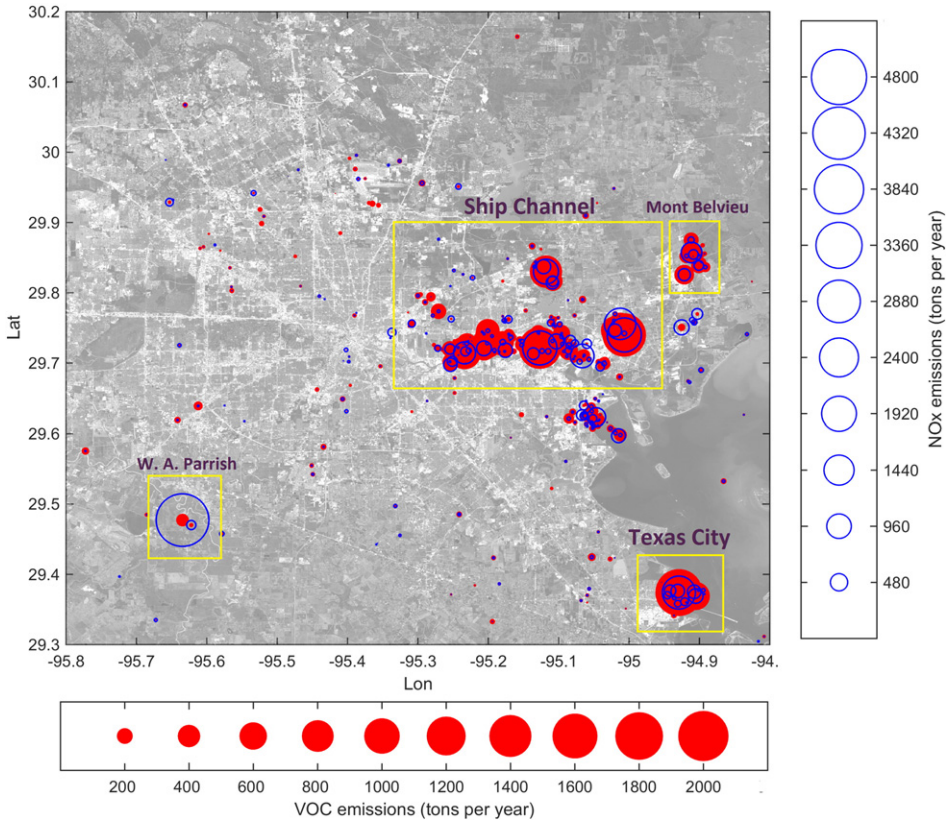

Fig. 2. Landsat8 imagery showing point emission sources in Houston from the Texas Commission on Environmental Quality 2013 PSEI. NO_x and VOC emissions are represented by open black circles and solid red circles, respectively, in units of tons per year. The Houston Ship Channel is home to the petrochemical industry, and W. A. Parrish is a power plant.

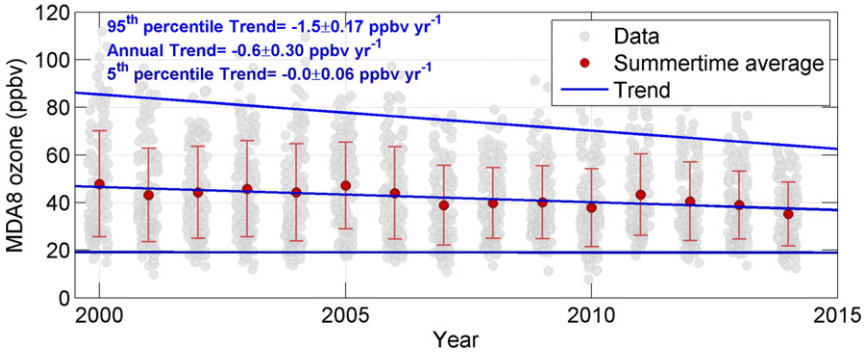

Fig. 3. The time series of MDA8 ozone from 11 CAMS observations during the summers of 2000 to 2014 in Houston, shown in solid gray circles. The solid red circles represent the means and the bars the mean and standard deviations for each year.

ozone precursors and/or changes in meteorology. If ozone and its precursors in Houston had indeed decreased, an investigation of the meteorological processes that may have been responsible for the changes would be of importance.

4.2. Clusters and their characteristics

To set up clustering, we defined two parameters: the number of clusters (k) and the number of Principal Components (PCs) (n). By changing one input (here k or n) while maintaining the other one constant, we used the grid-search method to compute a cost function. For this function we chose the silhouette index to investigate how well the clusters are separated. Consequently, we computed the index in a two-dimensional grid of (k,n) in the range of [(5,5),(40,15)] and then chose the (k,n) clusters with the highest values as the optima. For this work, we identified seven PCs (86% of variance) and ten clusters. One disadvantage of regional-based wind clustering was that some clusters showed distinctive patterns over the whole region while those in Houston remained the same. Based on our knowledge of the wind patterns in Houston and associated chemical characteristics, several clusters were combined resulting in seven clusters, which then became easier to interpret. As outlined earlier, we calculated 15 years of backward trajectories, conducted a CMAQ simulation, and used MDA8 CAMS observations (2000–2014). The results of our analysis of wind patterns, corresponding backward trajectories, and CAMS surface ozone observations are plotted in Fig. 4. The air pollutant levels (i.e., O_3 and NO_2) and relevant meteorological variables associated to the clusters (wind patterns) are listed in Table 2. The time coverage of the CAMS sites appearing in both Table 2 and Fig. 4 (95% of stations) is between 10 and 15 years. The simulated MDA8 surface for each cluster in summertime of 2014 (i.e., 150 days) is shown in Fig. 5. The definitions and descriptions of the patterns are included below:

4.2.1. Cluster 1 — Strong southerly or southeasterly

C1 included two sub-clusters. The first was associated with low pressure to the northwest and high pressure to the east and resulted in strong southeasterly and southerly winds, roughly similar to cluster 1 in Ngan and Byun (2011). The second pattern was associated with a strong and large high-pressure system located over the East Coast and the Atlantic. Generally, C1 was characteristic of strong southerly flow (warm and humid) ahead of a cold front with a low pressure located in the central plains and a high pressure located in the southeast United States. The winds were stronger in this cluster due to a strong pressure gradient between the high and low pressures. The location of the Bermuda High could explain the low-level jet of these southerly flows (Higgins et al., 1997). To investigate this potential impact, we calculated the Bermuda High Index (BHI) (Zhu and Liang, 2013) for the summers of 2000 to 2014 (i.e., May–September) by calculating the differences between the regional mean sea level pressure of the Gulf of Mexico and that of the southern Great Plains. When the BHI was positive, the pressure gradient force between the two regions became large, which in turn caused an increase in the low-level jet. The correlations between the BHI index and C1 (strong southerly winds) frequency was found +0.5. This means that the larger pressure gradient (i.e., higher BHI) partially contributed to the higher number of southerly winds. C1 was common in the months of May, June, and July, accounting for 16% of the total patterns. The backward trajectory frequencies indicated a predominately southeasterly wind. This cluster exhibited the lowest NO_2 and ozone concentrations, which resulted not only from clean marine O_3 transported into Texas from the Gulf but also a suppressed accumulation of local ozone and its precursors. Accordingly, less than 1% of the pattern days experienced ozone exceedances (MDA8 > 70 ppbv). Additionally, the model simulation and CAMS monitors thoroughly captured abnormally low ozone levels in summer.

4.2.2. Cluster 2 — moderate southerly and southwesterly

C2 was the largest cluster (41%), containing three sub-clusters with moderate southerly and southwesterly winds. C2 was characteristic of the wind pattern prior to a cold front passage with a low pressure located to the northwest and a high pressure located over the eastern Gulf of Mexico resulting in southerly or southwesterly winds in the HGB area. One sub-cluster was linked with high-pressure systems in the eastern U.S. and low-pressure systems in the southwestern U.S. In another sub-cluster, high-pressure systems in the Gulf, not far from the coast, resulted in southerly or southwesterly winds in the HGB area. The third sub-cluster was impacted by an extended high pressure system in the southeastern and eastern U.S. and the Atlantic. The C2 cluster was most common in the late spring and summer months from May to August. The trajectory analysis indicated a similar pattern for C1, but the air masses lingered over the Gulf during their short-range transport. Since the winds were weaker than the previous cluster, the surface ozone levels were comparatively higher.

4.2.3. Cluster 3 — weak northerly or northwesterly

C3 was associated with the wind pattern after a cold front had passed through the southern United States. Winds out of the north and northwest were associated with the passage of a cold front (comparatively lower temperature and relative humidity). From May to September (7%), the cold fronts were generally weak when they arrived in the southern states. As a result, local northwesterly winds were weak. The correlation between BHI and the frequency of this cluster was found −0.6 suggesting that the Bermuda High intensity contributed to reducing the likelihood of cold fronts. In addition, the frequency of the trajectory was combined with some southerly air masses, which may have been attributed to weak cold fronts and an abrupt transformation of this cluster into the C2 when the backward air masses arrived, for it was likely that a cold front occurred by the day after C2. The simulated MDA8 surface ozone and CAMS exhibited uniform levels in Houston.

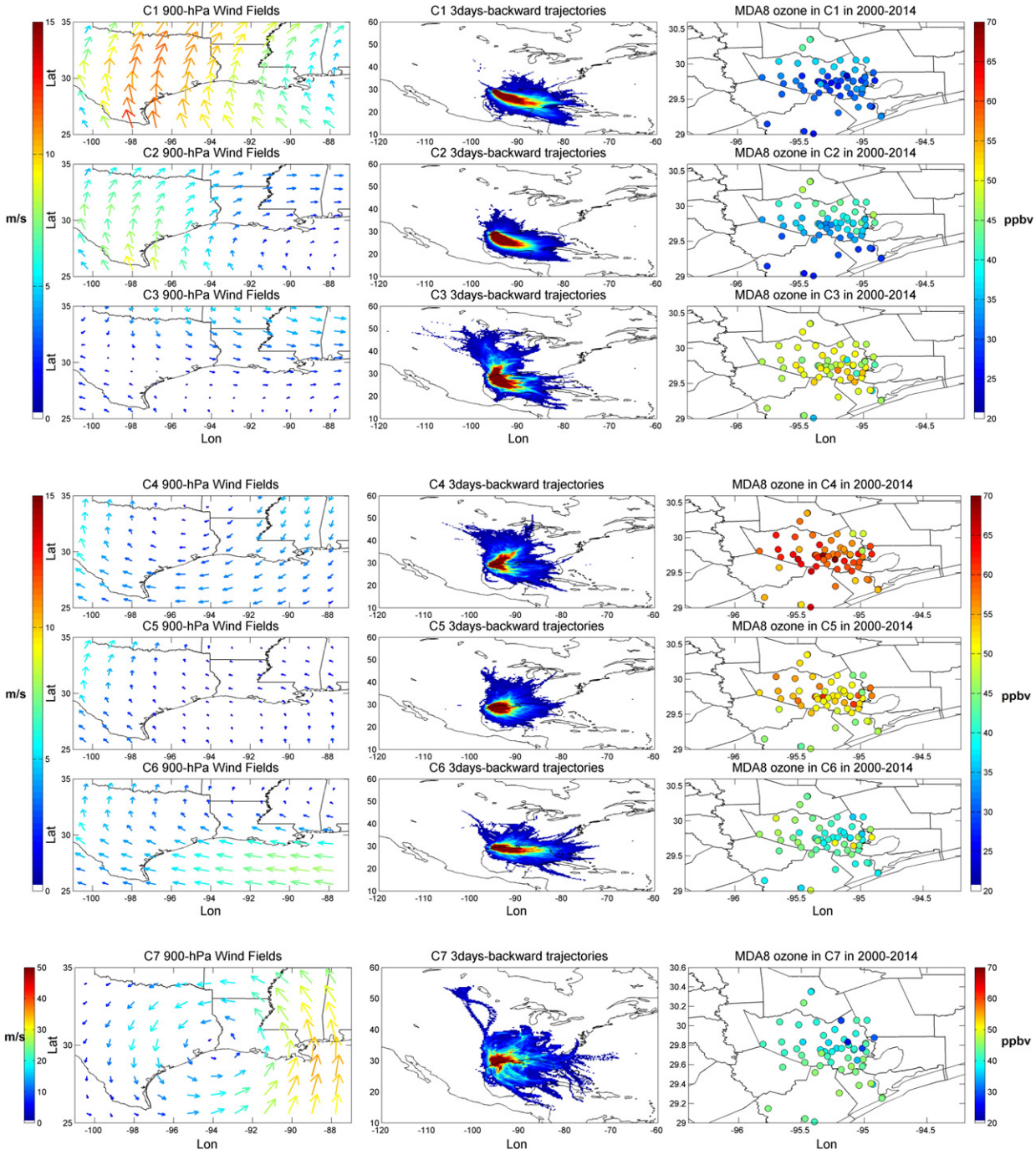

Fig. 4. Left panel: the mean values of 900-hPa wind fields from NARR for each cluster (red color represents stronger winds); middle panel: corresponding three-day backward trajectory frequency map arriving to CAMS stations (50 sites); right panel: surface MDA8 ozone from CAMS monitors.

4.2.4. Cluster 4 — weak easterly or northeasterly

C4 was associated with a high pressure that had moved in following the passage of the cold front. This high pressure is located over the south central plains, which means Houston has primarily easterly and northeasterly flow nearly coinciding with C5 in Ngan and Byun (2011). The frequency of this pattern was the same as that for C3 (7%). Backward trajectories were found more frequently in northeast and east of Houston. As shown before, most of the VOC (from petrochemical facilities) and NO_x emissions (from mobile sources) were located to the east and in the center of Houston, respectively. As a result, an easterly flow carried high levels of VOCs to the center of Houston that subsequently led to a marked increase in the rate of ozone production; therefore the days with the highest ozone exceedances reached 26% and the highest average ozone peak (107 ppbv) occurred in this cluster. The high ozone levels for this cluster were not only attributed to location of the Houston Ship Channel but the upwind ozone pollution from the Eastern United States (i.e., large regional background ozone) (Rappenglück et al., 2008). It appears that the corresponding CMAQ simulation and CAMS sites reported the higher ozone concentrations in this region than in the other clusters.

Table 2
The atmospheric chemical and meteorological characteristics of each cluster, measured by all available CAMS observations (parentheses denote standard deviations).

	C1	C2	C3	C4	C5	C6	C7
Number of days	351	918	187	188	331	212	65
Temperature (°F)	80 (4)	82 (6)	79 (5)	79 (5)	81 (3)	81 (6)	77 (4)
Max T (°F)	91 (5)	96 (6)	91 (7)	93 (5)	96 (5)	94 (6)	90 (5)
Std daily T (°F)	4	5	6	6	5	5	5
Relative humidity (%)	76 (6)	72 (7)	66 (6)	65 (7)	70 (8)	72 (6)	73 (5)
No. of ozone exceedances[a] (MDA8 > 70 ppbv)	1	48	19	48	65	14	1
Fraction of ozone exceedances (%)	<1%	5%	10%	26%	19%	7%	1%
Averaged ozone[b] (ppbv)	22 (9)	22 (10)	29 (10)	35 (9)	31 (10)	27 (9)	29 (7)
Maximum ozone[c] (ppbv)	57 (19)	76 (30)	89 (27)	107 (27)	98 (31)	77 (27)	67 (19)
Averaged peaks[d] (ppbv)	37 (13)	45 (16)	58 (16)	70 (16)	63 (19)	51 (17)	47 (13)
Averaged NO_2 (ppbv)	6 (3)	6 (2)	9 (2)	10 (3)	9 (3)	8 (3)	7 (1)
Maximum NO_2 (ppbv)	27 (12)	29 (19)	39 (16)	44 (14)	39 (15)	34 (12)	31 (15)
Averaged peaks NO_2 (ppbv)	13 (6)	14 (6)	20 (7)	23 (9)	20 (6)	18 (6)	15 (5)

[a] The number of high ozone days was calculated from averaged MDA8 ozone based on all stations which exceeded 70 ppbv. This threshold (70 ppbv) is based on the latest threshold of standard MDA8 ozone suggested by the Environmental Protection Agency.
[b] Averaged ozone and NO_2 included both daytime and nighttime observations.
[c] The maximum level was the highest values observed among the stations.
[d] Averaged peak was the mean of the 1-h max ozone of stations.

4.2.5. Cluster 5 — Weak winds

C5 (15%) presented several weather conditions that led to a weak circulation in the HGB area. This cluster was associated with an eastward movement of the high pressure and coincident change from easterly to southeasterly flow. Both C4 and C5 exhibit weaker wind speeds and favorable wind directions for ozone production; however due to location of Houston Ship Channel and the regional background ozone, C4 days comprise higher ozone levels than C5. The backward trajectories showed almost a circular pattern that is indicative of stagnant meteorological conditions conducive to ozone production, which resulted in 19% of the high-ozone days. In this case the model did not accurately simulate ozone, possibly because of the widely known uncertainties of emissions (Choi and Souri, 2015b) or overprediction of wind speed during stagnant conditions (e.g., Li et al., 2015).

4.2.6. Cluster 6 — moderate easterly or southeasterly

C6 was associated with strong easterly and southeasterly flow, which has resulted from an eastward shift of the high pressure and an increased pressure gradient. This occurred frequently in the month of September with a 9% frequency during the time of the study. The three-day backward trajectories revealed an elongated shape from the East. Despite the favorable direction of this flow for ozone production due to location of Houston Ship Channel, the magnitudes of the winds were high enough to disperse ozone precursors from the city. Consequently, only 7% of ozone exceedances were found within the C6 occurrence. Similar to C4, the days experiencing C6 pattern were likely to be affected by relatively high regional background ozone from the Eastern U.S. The CMAQ output for 2014 (Fig. 5) showed low overall levels of ozone in Houston. The transition of C6 to C1 will occur and the cycle of clusters (C1–C6) will repeat.

4.2.7. Cluster 7 — low pressure system

C7 contained exceptional low-pressure systems centered in various locations east or north of HGB region, which is similar to the A7 cluster reported by Davis et al. (1998). It had the lowest frequency among the clusters (3%). About half of the days of C7 were impacted by well-known hurricanes (e.g., Katrina). Depending on the exact location and strength of the low-pressure system, the winds in the HGB region varied from northerly to northwesterly to westerly. Several days impacted by cold fronts also fell into this cluster. As these storms (weak or strong) moved rapidly, the backward trajectory frequencies revealed a distorted shape. The unstable conditions associated with cloudy and rainy days led to low ozone concentrations.

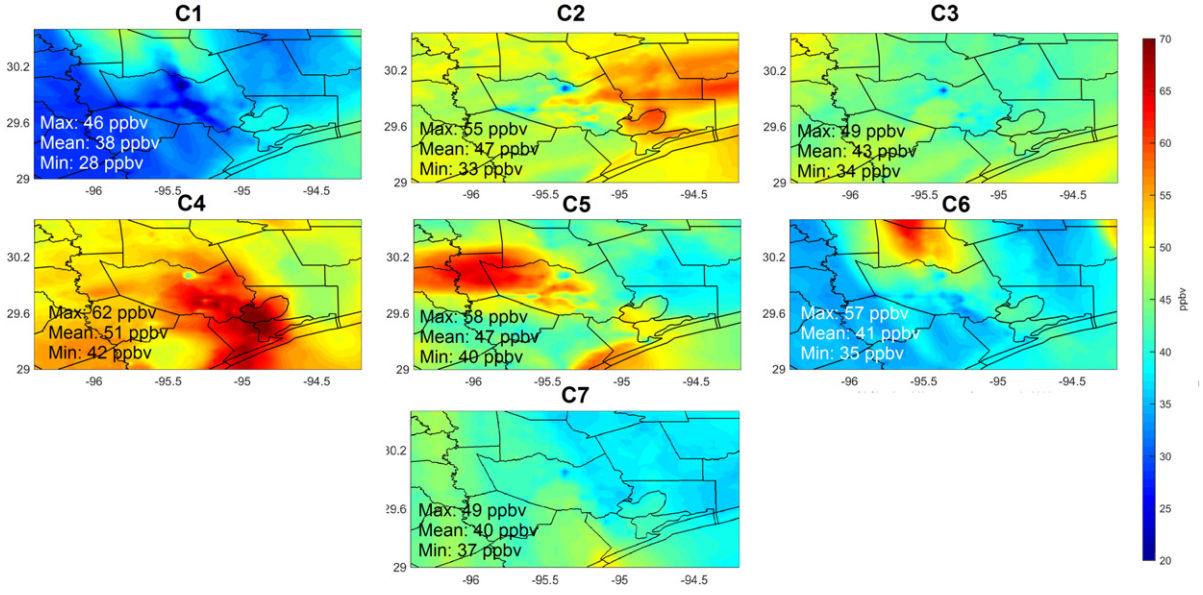

Fig. 5. Simulated MDA8 ozone for the days categorized in each cluster by using CMAQ. The time period is summertime 2014.

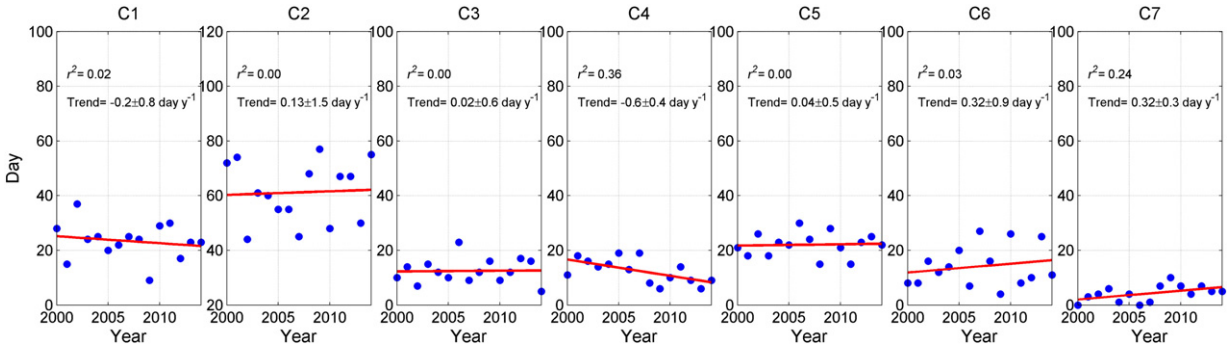

Fig. 6. The frequency of each cluster is shown in blue circles. The red lines represent the trends calculated from a linear trend, and the corresponding goodness of fit is shown.

4.3. Long-term cluster frequencies and patterns

For each year of the observation period (2000 to 2014), the summertime frequency of the seven main wind patterns was computed and presented in Fig. 6. To retrieve the trends we made use of a simple linear regression. Most of the clusters exhibited no evident trends. However, cluster 7 demonstrated an upward trend (0.3 ± 0.3 day yr^{-1}) which may not have been influential on ozone because of its low number of occurrences. Among the frequency changes a statistically significant downward trend for C4 (-0.6 ± 0.4 day yr^{-1}), the wind pattern with the highest ozone episodes, occurred. This is significant, since C4 has the highest fraction of ozone exceedances.

The time series of the number of days of averaged MDA8 ozone >70 ppbv along with C4 frequencies is depicted in Fig. 7. Results showed the number of ozone exceedances was trending downward (-1.5 ± 0.6 day yr^{-1}) during the period. As outlined earlier C4 days accounted for 26% of the ozone. This means that the C4 trend has the highest potential to impact the total number of ozone exceedances. Fig. 7 shows that both C4 and all of the ozone exceedances decreased by 82% and 87% since 2000. Figs. 6 and 7 demonstrate that the reduction in anthropogenic emissions was not the sole reason for the downward trend of ozone exceedances during the period. Our wind pattern clustering results showed a jump in the frequency of C4 in 2011, which was also observed during the days of ozone exceedances. This explained that in addition to experiencing a warmer year in 2011 (i.e., La Niña), the frequency of C4 days was also relatively high which consequently increased the number of ozone exceedances beyond the trend of year-to-year reduction.

4.4. Ozone trends in clusters

In this section, we will examine the trends of ozone in each cluster. This step not only provides information on ozone changes for each wind pattern but also paves the way for calculating both baseline and locally-produced ozone trends. Such a calculation is necessary since the effectiveness of emission controls can be determined when these quantities are measured. Fig. 8 depicts the time series of MDA8 ozone for each cluster, excluding C7 whose few occurrences prevented finding a statistically significant trend. Here we used all stations in the HGB region that measured more than 2100 days out of 2250 summertime days (i.e., 11 stations). We calculated the daily MDA8 for each station and then averaged it for all stations.

The magnitudes of NO_x and VOC anthropogenic emissions have significantly declined in Houston due to the implementation of emission control strategies. One way to quantify the impacts of anthropogenic emissions is to analyze the wind pattern responsible for the greatest impact of local emissions (i.e., C4 or C5) on ozone, even though the contributions of regional background ozone were always present, especially for C4. MDA8 ozone for C4 days is depicted in Fig. 8 showing a clear trend of relatively large reductions in the 95th (-1.5 ± 0.57 ppbv yr^{-1}) and 5th (-1.0 ± 0.49 ppbv yr^{-1}) percentiles and the summertime (-1.1 ± 0.47 ppbv yr^{-1}). The summertime trend for this cluster was found to be two times higher than the regional background ozone for northeasterly winds based on Berlin et al. (2013) who quoted -0.50 ± 0.54 ppbv yr^{-1} between 1998 and 2012. This suggested that local emission reductions could be responsible for at least ~50% reduction in ozone trends during C4. Fortunately, C5, which could not be impacted largely by regional background ozone, exhibited a significant

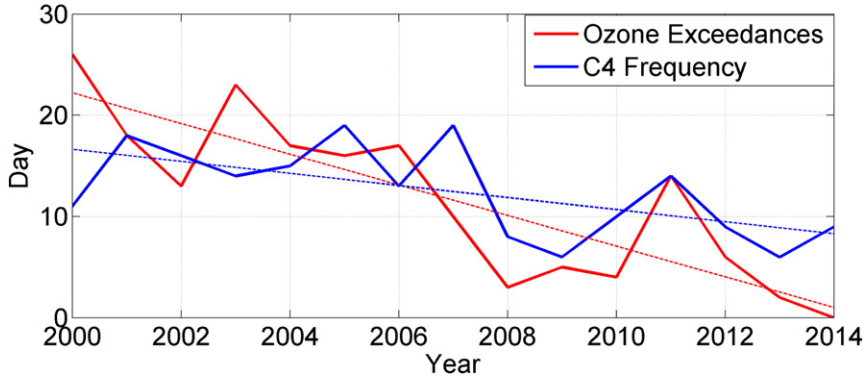

Fig. 7. The time series of days with ozone exceedances and the corresponding C4 frequency (weak easterly and northeasterly winds). Dashed lines are linear trends; they are found -1.5 ± 0.6 day yr^{-1} and -0.6 ± 0.4 day yr^{-1} for ozone exceedances and C4 frequency respectively.

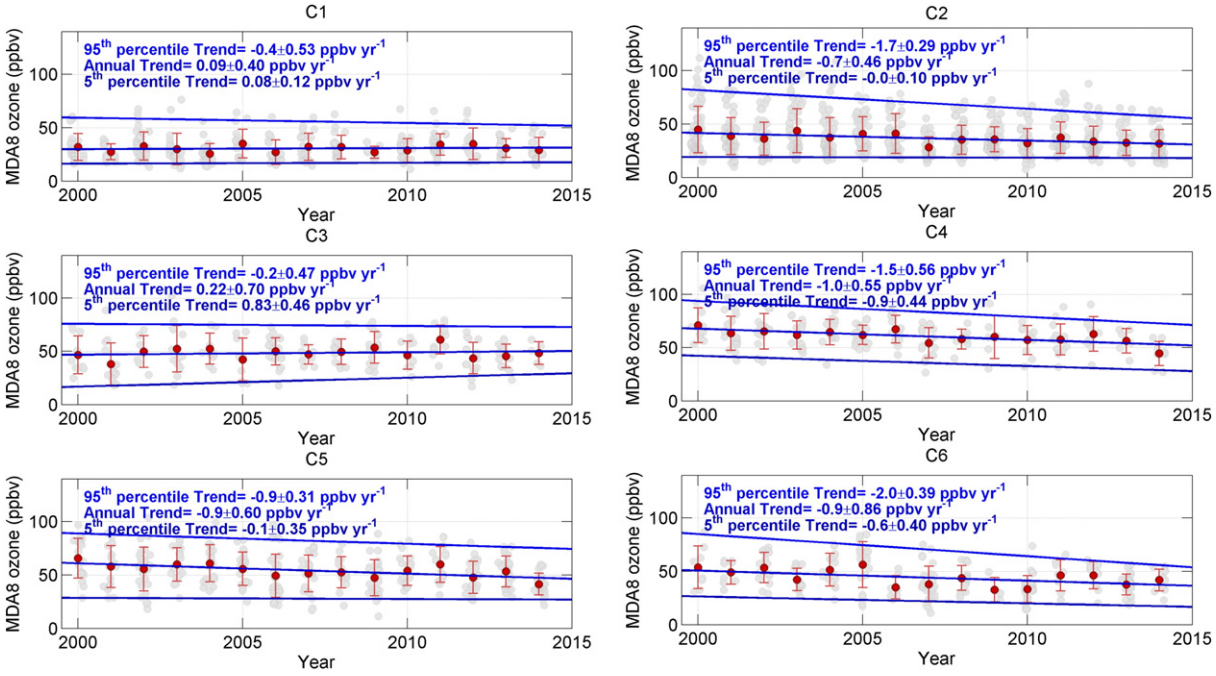

Fig. 8. Trends in the mean and 95th and 5th percentiles of MDA8 ozone in the summertime of 2000 to 2014 for each cluster. The average MDA8 of the 11 CAMS sites has been used, covering more than 93% of the time period. C4 and C5 mostly explain the variations in ozone governed by local emissions.

downward trend in both the 95th percentile and the summertime mean. This suggests that when the C5 condition occurred an ongoing reduction in anthropogenic emissions had mitigated ozone levels between 7 and 21 ppbv. Ozone within the C1 and C3 days did not show statistically significant trends; however, the upward trend of C3 in the 5th percentile was statistically significant (0.83 ± 0.49 ppbv yr^{-1}). Interestingly, C6 on average showed a considerable reduction in the 95th percentile and summertime ozone (but highly variable). The most probable reason for the reductions in C6 ozone trends could be the impact of regional background ozone from the Eastern U.S., since this wind pattern had the strongest wind speed carrying ozone from the region.

One way to calculate baseline ozone is to assume that NO_x and VOC levels were at their lowest values in the area and that marine O_3 transported into the city was dominant. This assumption was based on our belief that the city received the cleanest air from the strong southerly/southeasterly winds (C1) (e.g., Ngan and Byun, 2011). We did not account for moderate southerly winds (C2) because they only minimally push inland in northern regions, leaving ozone levels in some parts of Houston relatively unchanged. To capture a more relevant trend in baseline ozone, we changed MDA8 to daytime ozone when typically southerly/southeasterly wind (including synoptic and sea breeze) prevailed. To reduce the effect of recirculation (Banta et al., 2005), we removed days that had previously experienced C3 and analyzed only sites with latitudes lower than 29.5° (i.e., three stations). Fig. 9 depicts the time series of mean daytime ozone along with 95th and 5th percentiles, and the summertime trends. The summertime mean values generally indicated very low values (with mean of 24 ppbv), which was attributed to the presence of strong southerly winds. Due to the apparent variability of ozone in the Gulf and the time period of the study, C1 days showed on average no statistically significant trend of daytime ozone ($+0.2 \pm 0.3$ ppbv yr^{-1}). However, this trend was likely positive. While the 95th percentile trend and summertime trend were not statistically significant, the 5th percentile exhibited a statistically significant upward trend (0.14 ± 0.09 ppbv yr^{-1}) when the cleanest air prevailed. This demonstrated that the cleanest air masses that Houston received became more polluted over time by 1–3 ppbv.

5. Conclusions

This paper firstly provided up-to-date long-term trends of summertime surface ozone and NO_2 from CAMS observations in Houston; secondly, it used a classification approach to cluster 15 years of wind

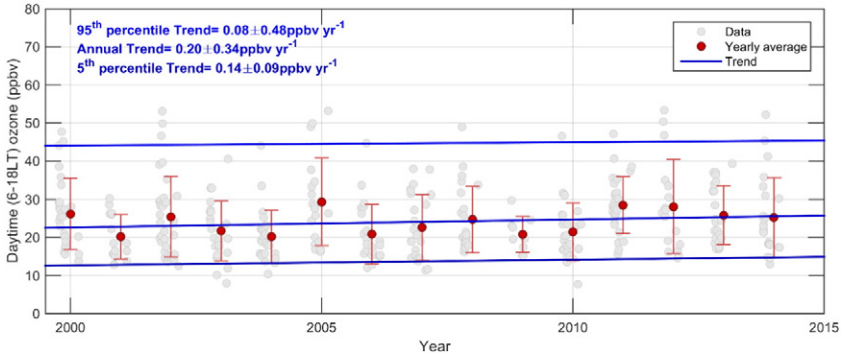

Fig. 9. The time series of daytime ozone from 3 CAMS observations (latitude <29.65°) during C1 in Houston shown in solid gray circles. The solid red circles represent the means and the bars the standard deviations for each summer.

directions from the NARR dataset and examined the statistical characteristics of each wind pattern on surface ozone and its respective changes; and thirdly, using information gathered about the wind patterns, it calculated the trends of baseline ozone from the Gulf of Mexico and that of ozone mostly from local emissions. This study differed from earlier studies on the same subject, in that the emphasis was on the long-term regional wind pattern impacts on surface ozone, the change in their frequencies, and the way to estimate ozone trends corresponding to local emission impacts and the Gulf of Mexico origins (i.e., baseline ozone). This paper presents the following broad conclusions:

1) The Houston Ship Channel plays a key role in ozone production in Houston. By using the TCEQ 1999 and 2013 PSEI emissions, we found that VOC point source emissions decreased by 44% in the region. Moreover, CAMS observations revealed that MDA8 NO_2 concentrations steadily decreased. The downward trend of MDA8 NO_2, -0.45 ± 0.04 ppbv yr^{-1} from May to September of 2000 to 2014 was expected as a result of improvements in fuel technology and decreased emissions from vehicles and point sources, which were attributed to effective control policies. The reduction in anthropogenic emissions might partially have led to the downward trend (-0.6 ± 0.3 ppbv yr^{-1}) of MDA8 ozone during the summertime.
2) We clustered the 2550 days of summertime from 2000 to 2014 based on the NARR wind field dataset and identified the chemical and physical characteristics corresponding to the clusters from more than 50 CAMS observations, a 15-year backward trajectory analysis, and a CMAQ simulation from 2014 summer. Based on the characteristics of each weather pattern, the following clusters associated with the fraction of ozone exceedances and averaged ozone were found: C1 (strong southerly or southeasterly, 1%, 37 ± 13 ppbv), C2 (moderate southerly, 5%, 45 ± 16 ppbv), C3 (northerly or northwesterly, 10%, 58 ± 16 ppbv), C4 (weak easterly or northeasterly, 26%, 70 ± 16 ppbv), C5 (weak winds, 19%, 63 ± 19 ppbv), C6 (moderate easterly or southeasterly, 7%, 51 ± 17 ppbv), and C7 (low-pressure system, 1%, 47 ± 13 ppbv). The highest ozone level belonged to C4 days, when weak easterly and northeasterly winds mixed high VOC emissions from the Houston Ship Channel with NO_x emissions from the urban area, in addition to the transported ozone from the Eastern United States. While a dominant high-pressure system, intensive solar radiation, and very weak winds in C5 had been expected to produce higher ozone concentrations, emissions from the Houston Ship Channel created more pollution in C4. The cleanest conditions were in C1, when Houston received relatively clean air masses from the Gulf of Mexico.
3) The long-term frequency trends of clusters, except for C4 and C7, which showed -0.6 ± 0.4 day yr^{-1} and 0.3 ± 0.3 day yr^{-1} trends respectively, were highly variable in the summers. The declining trend in C4 (82% in respect to 2000) provided evidence that the reduction in anthropogenic sources was not the only reason for the reduction in ozone exceedances (-1.5 ± 0.6 day yr^{-1}; 87% reduction in respect to 2000).
4) We examined the MDA8 ozone trends in each cluster. C2, C4, C5, and C6 exhibited a large reduction in the 95th percentile and summertime values during the study period. In particular, the summertime ozone trend for C4 was two times greater than the regional background ozone for northeasterly winds reported in Berlin et al. (2013). Additionally, ozone trends for C5, which marginally were impacted by regional background ozone, showed large downward trends. These results indicate that besides decreasing trends in C4 frequencies, the decrease in anthropogenic emissions also led to a decrease in ozone concentrations over Houston. Finally, using the three southeastern CAMS sites, we calculated the trend in daytime surface ozone in the C2 cluster. We found the 5th percentile, with the lowest summertime ozone levels in Houston, exhibited a statistically significant upward trend (0.14 ± 0.09 ppbv yr^{-1}) suggesting that the cleanest air masses that Houston received became more polluted by 1–3 ppbv.

In summary, this work suggests that wind pattern clustering in a long-term period is a powerful tool to track ozone changes. Future applications of this will include simulations of climate scenarios to understand the effect of wind pattern change on air quality.

Acknowledgments

We express our sincere appreciation to Rebecca Washenfelder for providing the point source information. NARR data provided by the NOAA-ESRL Physical Sciences Division in Boulder, Colorado, from their website at http://www.esrl.noaa.gov/psd/data/gridded/data.narr.html. We also show other thanks to Yuxuan Wang at Texas A&M University Galveston and Fantine Ngan at NOAA ARL for their useful comments on BHI and PCA/clustering analysis, respectively. MACCity emissions were retrieved from http://eccad.sedoo.fr/.

References

Banta, R.M., Senff, C.J., Nielsen-Gammon, J., Darby, L.S., Ryerson, T.B., Alvarez, R.J., Sandberg, S.P., Williams, E.J., Trainer, M., 2005. A bad air day in Houston. Bull. Am. Meteorol. Soc. 86, 657–669.

Berlin, S.R., Langford, A.O., Estes, M., Dong, M., Parrish, D.D., 2013. Magnitude, decadal changes, and impact of regional background ozone transported into the greater Houston, Texas area. Environ. Sci. Technol. 47 (24), 13985–13992.

Byun, D., Schere, K.L., 2006. Review of the governing equations, computational algorithms, and other components of the models—3 Community Multiscale Air Quality (CMAQ) modeling system. Appl. Mech. Rev. 59 (2), 51–77.

Chan, E., Vet, R.J., 2010. Baseline levels and trends of ground level ozone in Canada and the United States. Atmos. Chem. Phys. 10 (18), 8629–8647.

Choi, Y., 2014. The impact of satellite-adjusted NO_x emissions on simulated NO_x and O_3 discrepancies in the urban and outflow areas of the Pacific and Lower Middle US. Atmos. Chem. Phys. 14 (2), 675–690.

Choi, Y., Souri, A.H., 2015a. Seasonal behavior and long-term trends of tropospheric ozone, its precursors and chemical conditions over Iran: a view from space. Atmos. Environ. 106, 232–240.

Choi, Y., Souri, A.H., 2015b. Chemical condition and surface ozone in large cities of Texas during the last decade: observational evidence from OMI, CAMS, and model analysis. Remote Sens. Environ. 168, 90–101.

Choi, Y., Kim, H., Tong, D., Lee, P., 2012. Summertime weekly cycles of observed and modeled NO_x and O_3 concentrations as a function of satellite-derived ozone production sensitivity and land use types over the Continental United States. Atmos. Chem. Phys. 12, 6291–6307.

Cooper, O.R., Gao, R.-S., Tarasick, D., Leblanc, T., Sweeney, C., 2012. Long-term ozone trends at rural ozone monitoring sites across the United States, 1990–2010. J. Geophys. Res. 117, D22.

Czader, B.H., Choi, Y., Li, X., Alvarez, S., Lefer, B., 2015. Impact of updated traffic emissions on HONO mixing ratios simulated for urban site in Houston, Texas. Atmos. Chem. Phys. 15 (3), 1253–1263.

Darby, L.S., 2005. Cluster analysis of surface winds in Houston, Texas, and the impact of wind patterns on ozone. J. Appl. Meteorol. 44 (12), 1788–1806.

Davis, J.M., Eder, B.K., Nychka, D., Yang, Q., 1998. Modeling the effects of meteorology on ozone in Houston using cluster analysis and generalized additive models. Atmos. Environ. 32 (14), 2505–2520.

De Smedt, I., Stavrakou, T., Hendrick, F., Danckaert, T., Vlemmix, T., Pinardi, G., Theys, N., Lerot, C., Gielen, C., Vigouroux, C., Hermans, C., Fayt, C., Veefkind, P., Müller, J.-F., Van Roozendael, M., 2015. Diurnal, seasonal and long-term variations of global formaldehyde columns inferred from combined OMI and GOME-2 observations. Atmos. Chem. Phys. 15, 12519–12545. http://dx.doi.org/10.5194/acp-15-12519-2015.

De Smedt, I., Stavrakou, T., Müller, J.-F., van der A, R.J., Van Roozendael, M., 2010. Trend detection in satellite observations of formaldehyde tropospheric columns. Geophys. Res. Lett. 37, L18808. http://dx.doi.org/10.1029/2010GL044245.

Duncan, B.N., Lamsal, L.N., Thompson, A.M., Yoshida, Y., Lu, Z., Streets, D.G., Hurwitz, M.M., Pickering, K.E., 2016. A space-based, high-resolution view of notable changes in urban NOx pollution around the world (2005–2014). J. Geophys. Res. http://dx.doi.org/10.1002/2015JD024121.

Fu, T.M., Zheng, Y., Paulot, F., Mao, J., Yantosca, R.M., 2015. Positive but variable sensitivity of August surface ozone to large-scale warming in the southeast United States. Nat. Clim. Chang. 5, 454–458.

Higgins, R.W., Yao, Y., Yarosh, E.S., Janowiak, J.E., Mo, K.C., 1997. Influence of the Great Plains low-level jet on summertime precipitation and moisture transport over the central United States. J. Clim. 10 (3), 481–507.

Hilboll, A., Richter, A., Burrows, J.P., 2013. Long-term changes of tropospheric NO_2 over megacities derived from multiple satellite instruments. Atmos. Chem. Phys. 13, 4145–4169. http://dx.doi.org/10.5194/acp-13-4145-2013.

Hong, S.Y., Noh, Y., Dudhia, J., 2006. A new vertical diffusion package with an explicit treatment of entrainment processes. Mon. Weather Rev. 134 (9), 2318–2341.

Huang, L., McGaughey, G., McDonald-Buller, E., Kimura, Y., Allen, D.T., 2015. Quantifying regional, seasonal and interannual contributions of environmental factors on isoprene and monoterpene emissions estimates over eastern Texas. Atmos. Environ. 106, 120–128.

Huth, R., Beck, C., Philipp, A., Demuzere, M., Ustrnul, Z., Cahynová, M., Tveito, O.E., 2008. Classifications of atmospheric circulation patterns. Ann. N. Y. Acad. Sci. 1146 (1), 105–152.

Jobson, B.T., Berkowitz, C.M., Kuster, W.C., Goldan, P.D., Williams, E.J., Fesenfeld, F.C., Apel, E.C., Karl, T., Lonneman, W.A., Riemer, D., 2004. Hydrocarbon source signatures in Houston, Texas: influence of the petrochemical industry. J. Geophys. Res. 109, D24305. http://dx.doi.org/10.1029/ 2004JD004887.

Kemball-Cook, S., Parrish, D., Ryerson, T., Nopmongcol, U., Johnson, J., Tai, E., Yarwood, G., 2009. Contributions of regional transport and local sources to ozone exceedances in Houston and Dallas: comparison of results from a photochemical grid model to aircraft and surface measurements. J. Geophys. Res. 114, D7.

Koenker, R., Hallock, K., 2001. Quantile regression: an introduction. J. Econ. Perspect. 15 (4), 43–56.

Lamarque, J.-F., Bond, T.C., Eyring, V., Granier, C., Heil, A., Klimont, Z., Lee, D., Liousse, C., Mieville, A., Owen, B., Schultz, M.G., Shindell, D., Smith, S.J., Stehfest, E., Van Aardenne, J., Cooper, O.R., Kainuma, M., Mahowald, N., McConnell, J.R., Naik, V., Riahi, K., van Vuuren, D.P., 2010. Historical (1850–2000) gridded anthropogenic and biomass burning emissions of reactive gases and aerosols: methodology and application. Atmos. Chem. Phys. 10, 7017–7039. http://dx.doi.org/10.5194/acp-10-7017-2010.

Lefer, B., Rappenglück, B., Flynn, J., Haman, C., 2010. Photochemical and meteorological relationships during the Texas-II Radical and Aerosol Measurement Project (TRAMP). Atmos. Environ. 44 (33), 4005–4013.

Lefohn, A.S., Shadwick, D., Oltmans, S.J., 2010. Characterizing changes in surface ozone levels in metropolitan and rural areas in the United States for 1980–2008 and 1994–2008. Atmos. Environ. 44, 5199–5210.

Li, J., Yang, W., Wang, Z., Chen, H., Hu, B., Li, J., Sun, Y., Fu, P., Zhang, Y., 2016. Modeling study of surface ozone source–receptor relationships in East Asia. Atmos. Res. 167, 77–88.

Li, X., Choi, Y., Czader, B., Kim, H., Lefer, B., Pan, S., 2015. The impact of observation nudging on simulated meteorology and ozone concentrations during DISCOVER-AQ 2013 Texas campaign. Atmos. Chem. Phys. Discuss. 15 (19), 27357–27404.

Lin, M., Fiore, A.M., Horowitz, L.W., Langford, A.O., Oltmans, S.J., Tarasick, D., Rieder, H.E., 2015. Climate variability modulates western US ozone air quality in spring via deep stratospheric intrusions. Nat. Commun. 6.

Mesinger, F., DiMego, G., Kalnay, E., Mitchell, K., Shafran, P.C., W., Ebisuzaki, Jović, D., Woollen, J., Rogers, E., Berbery, E.H., Ek, M.B., Fan, Y., Grumbine, R., Higgins, W., Li, H., Lin, Y., Manikin, G., Parrish, D., Shi, W., 2006. North American regional reanalysis. Bull. Am. Meteorol. Soc. 87 (3), 343–360.

Ngan, F., Byun, D., 2011. Classification of wind patterns and associated trajectories of high-ozone episodes in the Houston–Galveston–Brazoria area during the 2005/06 TexAQS-II. J. Appl. Meteorol. Climatol. 50 (3), 485–499.

Pan, S., Choi, Y., Roy, A., Li, X., Joen, W., Souri, A.-H., 2015. Modeling the uncertainty of several VOC and its impact on simulated VOC and ozone in Houston, Texas. Atmos. Environ. 120, 404–416.

Rappenglück, B., Perna, R., Zhong, S., Morris, G.A., 2008. An analysis of the vertical structure of the atmosphere and the upper-level meteorology and their impact on surface ozone levels in Houston, Texas. J. Geophys. Res. 113 (D17).

Russell, A.R., Valin, L.C., Cohen, R.C., 2012. Trends in OMI NO_2 observations over the United States: effects of emission control technology and the economic recession. Atmos. Chem. Phys. 12 (24), 12197–12209.

Seinfeld, J.H., Pandis, S.N., 2012. Atmospheric Chemistry and Physics: From Air Pollution to Climate Change. John Wiley & Sons.

Sillman, S., 1995. The use of NOy H2O2, and HNO3 as indicators for ozone–NOx–hydrocarbon sensitivity in urban locations. J. Geophys. Res. 100 (D7), 14–175.

Simon, H., Reff, A., Wells, B., Xing, J., Frank, N., 2014. Ozone trends across the United States over a period of decreasing NOx and VOC emissions. Environ. Sci. Technol. 49 (1), 186–195.

Skamarock, W.C., Klemp, J.B., 2008. A time-split nonhydrostatic atmospheric model for weather research and forecasting applications. J. Comput. Phys. 227 (7), 3465–3485.

Souri, A.H., Vajedian, S., 2015. Dust storm detection using random forests and physical-based approaches over the Middle East. J. Earth. Syst. Sci. 124 (5), 1127–1141.

Souri, A.H., Choi, Y., Jeon, W., Li, X., Pan, P., Diao, L., Westenbarger, D.A., 2016. Constraining NOx Emissions Using Satellite NO_2 Measurements during 2013 DISCOVER-AQ Texas Campaign. http://dx.doi.org/10.1016/10.1016/j.atmosenv.2016.02.020 (in press).

Stein, A.F., Draxler, R.R., Rolph, G.D., Stunder, B.J.B., Cohen, M.D., Ngan, F., 2015. NOAA's HYSPLIT atmospheric transport and dispersion modeling system. Bull. Amer. Meteor. Soc. 96 (12), 2059–2077.

Tong, D.Q., Lamsal, L., Pan, L., Ding, C., Kim, H., Lee, P., Stajner, I., 2015. Long-term NO_x trends over large cities in the United States during the Great Recession: comparison of satellite retrievals, ground observations, and emission inventories. Atmos. Environ. 107, 70–84. http://dx.doi.org/10.1016/j.atmosenv.2015.01.035.

U.S. Environmental Protection Agency, U.S., 2014. Air Pollutant Emissions Trends Data. Avaiable at http://www.epa.gov/air-emissions-inventories/air-pollutant-emissions-trends-data.

Washenfelder, R.A., Trainer, M., Frost, G.J., Ryerson, T.B., Atlas, E.L., de Gouw, J.A., Flocke, F.M., Fried, A., Holloway, J.S., Parrish, D.D., Peischl, J., Richter, D., Schauffler, S.M., Walega, J.G., Warneke, C., Weibring, P., Zheng, W., 2010. Characterization of NO_x, SO_2, ethene, and propene from industrial emission sources in Houston, Texas. J. Geophys. Res. 115, D16311. http://dx.doi.org/10.1029/2009JD013645.

Zhou, W., Cohan, D.S., Henderson, B.H., 2014. Slower ozone production in Houston, Texas following emission reductions: evidence from Texas Air Quality Studies in 2000 and 2006. Atmos. Chem. Phys. 14 (6), 2777–2788.

Zhu, J., Liang, X.Z., 2013. Impacts of the Bermuda High on regional climate and ozone over the United States. J. Clim. 26 (3), 1018–1032.